

Risk-bounded Path Planning for Urban Air Mobility Operations under Uncertainty

Pengcheng Wu, Junfei Xie, Yanchao Liu and Jun Chen

Abstract—Collision avoidance is an essential concern for the autonomous operations of aerial vehicles in dynamic and uncertain urban environments. This paper introduces a risk-bounded path planning algorithm for unmanned aerial vehicles (UAVs) operating in such environments. This algorithm advances the rapidly-exploring random tree (RRT) with chance constraints to generate probabilistically guaranteed collision-free paths that are robust to vehicle and environmental obstacle uncertainties. Assuming all uncertainties follow Gaussian distributions, the chance constraints are established through converting dynamic and probabilistic constraints into equivalent static and deterministic constraints. By incorporating chance constraints into the RRT algorithm, the proposed algorithm not only inherits the computational advantage of sampling-based algorithms but also guarantees a probabilistically feasible flying zone at every time step. Simulation results show the promising performance of the proposed algorithm.

Index Terms—UAV, Path Planning, Chance Constraints, Urban Air Mobility

I. INTRODUCTION

Enabled by the technological advancements in automation, electrification and vertical take-off and landing, autonomous applications using a team of unmanned aerial vehicles (UAVs) in urban aviation, such as passenger mobility [1] and goods delivery [2], are drawing increasing attentions in recent years. However, the development of these applications still faces many challenges, among which safe flying is one of the most critical concerns for the successful operation. For safe and reliable operations, the requirement of collision avoidance should be fulfilled in path planning of autonomous vehicles [3], [4]. However, the existence of various types of uncertainties in real scenarios may cause UAV operations determined based on the current collision avoidance system to fail. To address this challenge, we propose to generate probabilistically guaranteed feasible paths for the UAVs at a given risk level of collision subject to different forms of uncertainties. To realize this strategy, it is critical to find the right balance between the planning trajectory’s safety and efficiency. In this paper, we develop a novel risk-bounded path planning algorithm that generates probabilistically guaranteed collision-free paths for a team of UAVs under uncertainties.

P. Wu is with the Department of Mechanical and Aerospace Engineering, University of California San Diego, La Jolla, CA 92093, and also with the Department of Aerospace Engineering, San Diego State University, San Diego, CA 92182 pwu@sdsu.edu, pcwupat@ucsd.edu

J. Xie is with the Department of Electrical and Computer Engineering, San Diego State University, San Diego, CA 92182, USA jxie4@sdsu.edu

Y. Liu is with the Department of Industrial & Systems Engineering, Wayne State University, Detroit, MI, USA yanchaoliu@wayne.edu

J. Chen (corresponding author) is with the Department of Aerospace Engineering, San Diego State University, San Diego, CA 92182, USA jun.chen@sdsu.edu

Two types of uncertainties are usually found in path planning scenarios involving collision avoidance [5]–[8]. One is vehicle uncertainty, which arises from factors like the inaccurate measurement of self-position or disturbance of wind and it is associated with each UAV in the team. The other is obstacle uncertainty, which is caused by the inaccuracy of UAVs’ onboard sensors and is associated with each obstacle to be evaded by all UAVs. To address vehicle uncertainty, Prentice et al. considered a linear system subject to Gaussian process noise to achieve the desired probability of feasibility [9]. Pepy et al. sought guaranteed feasibility for a nonlinear system subject to bounded state uncertainty of the vehicle [10]. In addition to vehicle uncertainty, many existing works have also focused on the obstacle uncertainty. Luders et al. studied probabilistic robustness to both process noise and uncertain dynamic obstacles following deterministic trajectories [11]. However, these works treated vehicle uncertainty and obstacle uncertainty separately, which made design and analyses complicated. In this paper, we introduce the transformation of relative uncertainty, which reduces different forms of uncertainty into a common one.

For a single UAV operating in a complex environment, one effective way to achieve balance between the planning conservatism and efficiency is through formulating the probabilistic bound for collision with obstacles as the chance constraints, meaning that the probability of constraint violation does not exceed a prescribed threshold [12], [13]. This can be achieved by converting probabilistic constraints into equivalent deterministic ones through a transformation. In previous studies, Blackmore et al. proposed a chance constraints formulation for a system subject to Gaussian noise, by assuming that all environmental obstacles have static and deterministic locations [14], [15]. Toit et al. developed a chance constrained framework that considered other types of uncertainties [16]. Luders et al. extended the chance constraints formulation to allow for dynamic and probabilistic obstacles [11]. Manuel et al. restricted each polyhedral obstacle to be a cuboid and then obtained a tight quadratic bound for collision avoidance analytically [17]. However, these existing chance constraints formulations considered approximation and therefore sacrificed the efficiency of path planning. In contrast, we propose a different chance constraints formulation in this paper. It applies to both vehicle and environmental obstacle uncertainties and is more efficient than existing methods while maintaining the same level of safety guarantee.

Path planning for multiple UAVs in a complex environment has also been investigated. A team of UAVs is able to accomplish multiple tasks in parallel and perform far more complicated tasks than a single UAV operating alone. Compared with a single UAV, the path planning for a team of UAVs

needs to consider not only the collisions with environmental obstacles but also the collisions among the UAVs [18]. To address this challenge, Scerri et al. proposed a deconfliction strategy in which the team must reach a consensus on path feasibility for any updated path [19]. Another remarkable approach was proposed by Purwin et al., in which vehicles reserve regions of the map to move in and must reach a consensus on any modifications to these regions [20]. Desaraju et al. proposed an algorithm for multi-vehicle systems with complex constraints [21]. However, in the aforementioned studies, either the vehicles in the team or environmental obstacles are assumed to be deterministic, which is a strong assumption in realistic operations. In this paper, we propose a more advanced path planning algorithm, extended from the rapidly-exploring random tree (RRT), for a team of UAVs operating in complex environments under both vehicle and environmental obstacle uncertainties.

The RRT is an incremental sampling-based algorithm designed for solving path planning problems that involve obstacles [5], [22]. It implements collision checking for widespread sampling points in the state space. Different from computationally intensive optimization approaches such as mixed-integer linear programs or constrained nonlinear programs which scale poorly with the number of constraints imposed by the complex environment, the RRT can efficiently model complex dynamics and constraints. However, the original RRT doesn't consider the chance constraints within its formulation, leading to the consequence that it cannot be used to directly deal with obstacles whose locations are uncertain. To break through this limitation, we incorporate chance constraints into the RRT formulation. The resulting method not only inherits the computational advantage of sampling-based algorithms, but also guarantees probabilistic feasibility for the planned path at every time step.

In this paper, we first propose an efficient chance constraints formulation which applies to both vehicle-obstacle and inter-vehicle collision avoidance. It can handle both vehicle uncertainty and obstacle uncertainty through the transformation of relative uncertainty by assuming that all location variables follow Gaussian distributions. Then, an extended RRT that incorporates the proposed chance constraints is developed, which ensures the probabilistic feasibility for the planned paths.

The remaining part of the article is organized as follows. In section II, the problem statement is presented. In section III, an efficient chance constraints formulation is proposed and fully discussed. In section IV, the chance constraints formulation is incorporated into the RRT development, with an updated planning order strategy developed. In section V, the feasibility of the proposed algorithm is verified through simulation cases. Finally, we conclude this article in section VI.

II. PROBLEM STATEMENT

Uncertainty is a major concern when it comes to the path planning of urban air mobility. For an aerial vehicle, its location \mathbf{x}_t at a particular time t may not be deterministic, due to vehicle uncertainty arising from factors like the inaccurate measurement

of self-position or disturbance of wind. Especially, under the assumption of Gaussian distribution, the location \mathbf{x}_t obeys

$$\mathbf{x}_t \sim \mathcal{N}(\boldsymbol{\mu}_{t*}, \boldsymbol{\Sigma}_*) \quad (1)$$

where $\mathcal{N}(\boldsymbol{\mu}_{t*}, \boldsymbol{\Sigma}_*)$ represents a Gaussian distribution with a time-varying mean $\boldsymbol{\mu}_{t*}$ and a time-invariant covariance $\boldsymbol{\Sigma}_*$.

To operate safely in a dynamic environment, each vehicle should avoid the environmental obstacles and other vehicles in the team. This can be achieved by introducing the following constraints

$$\mathbf{x}_t \notin \mathcal{X}_t \quad \forall t \quad (2)$$

$$\text{where } \mathcal{X}_t := \left(\bigcup_{i=1}^N \mathcal{X}_{ti} \right) \quad (3)$$

In the above constraints, we use \mathcal{X}_{ti} to denote the area in which obstacle i may be located at time t due to vehicle uncertainty, where $i \in \{1, 2, \dots, N\}$ and N is the total number of obstacles. We call such area as the **possible region** for obstacle i at time t . Note that, from the perspective of a particular vehicle, all the other vehicles in the team are also viewed as obstacles. It is also worth noting that the time dependence of \mathcal{X}_t allows the inclusion of either static or dynamic obstacles. In fact, for a particular vehicle in the team, all the other vehicles need to be modeled as dynamic obstacles, while the environmental obstacles might be static or dynamic.

From a given vehicle's perspective, the possible region of an obstacle i at time step t is modeled by the following equation, by assuming Gaussian uncertainty,

$$\begin{aligned} \mathcal{X}_{ti} &= \{ \mathbf{x} \in \mathbb{R}^d \mid \| \mathbf{x} - \mathbf{c}_{ti} \| \leq r_i \} \quad \forall t, i. \\ \mathbf{c}_{ti} &\sim \mathcal{N}(\boldsymbol{\mu}_{ti}, \boldsymbol{\Sigma}_i) \end{aligned} \quad (4)$$

where r_i is the minimum safety range for the vehicle to stay away from the i th obstacle to ensure safety, which depends on the speed of the obstacle [23]. In this paper, for simplicity, we assume r_i is constant at any time t . Additionally, \mathbf{c}_{ti} represents the position of the i th obstacle at time t , which is an independent Gaussian random variable, i.e., $\mathbf{c}_{ti} \sim \mathcal{N}(\boldsymbol{\mu}_{ti}, \boldsymbol{\Sigma}_i)$ with a time-varying mean $\boldsymbol{\mu}_{ti}$ and a time-invariant covariance $\boldsymbol{\Sigma}_i$. In cases of static obstacles, $\boldsymbol{\mu}_{ti} = \boldsymbol{\mu}_i$. Note that this formulation applies to both single- and multi-UAV systems.

Definition 1 (Collision Condition) A collision event happens when the vehicle is too close to an obstacle i , i.e.,

$$\| \mathbf{x}_t - \mathbf{c}_{ti} \| \leq r_* + r_i \quad (5)$$

where \mathbf{x}_t and \mathbf{c}_{ti} are the location of the vehicle and the obstacle at time t , respectively. r_* and r_i are their safety ranges. Note that both \mathbf{x}_t and \mathbf{c}_{ti} are random variables, therefore (4) corresponds to an event, denoted by *collision*, in the probability space.

Given the collision condition defined above, this paper aims to find probabilistically guaranteed collision-free paths for a set of UAVs to reach their target locations, such that the probability of collision with any obstacle at any time is smaller than a certain threshold, i.e.,

$$\Pr(\text{collision}) \leq \alpha \quad (6)$$

where α is a prescribed threshold, called risk level.

III. CHANCE CONSTRAINTS FORMULATION

In this section, we aim to quantify the probability of a vehicle to avoid collision with static or dynamic obstacles under both vehicle and obstacle uncertainty. Firstly, we study a simple case where the safety range of the vehicle and obstacle is negligible. In this case, we transform the possible region \mathcal{X}_{ti} in eq. (4) into a risk domain \mathcal{D}_{ti} at a given risk level α (or a confidence level $1 - \alpha$), which proves to be a circle or an ellipse. This allows probabilistic constraints to be represented as equivalent deterministic constraints. Based on this equivalent deterministic constraints, we further discuss the general case when safety range is non-negligible. Finally, we introduce the transformation of relative uncertainty to reduce both vehicle uncertainty and obstacle uncertainty into a common form of uncertainty to simplify the process of feasibility checking for the probabilistic bounds.

A. Chance Constraints for a Single Uncertain Obstacle

In this subsection, we consider a single obstacle subject to uncertainty, and derive the chance constraint for a vehicle to avoid this obstacle within a certain risk level α . The vehicle's location \mathbf{x}_t is assumed to be deterministic and the safety range for both the obstacle and the vehicle is assumed to be negligible (close to zero), i.e. $r_i = r_* := \delta \rightarrow 0$. For the general case of multiple obstacles and non-negligible safety range, we will discuss in section III-B and section III-C.

To obtain the chance constraint, we first find the risk domain of a d -dimensional Gaussian random variable in Lemma 1.

Definition 2 (Risk Domain) A set $\mathcal{D} \subset \mathbb{R}^d$ that satisfies

$$\Pr(\mathbf{X} \in \mathcal{D}) \geq 1 - \alpha \quad (7)$$

is called a risk domain at risk level α of a random variable \mathbf{X} .

Lemma 1 Let $\mathbf{X} \in \mathbb{R}^d$ be a d -dimensional random variable that obeys a d -dimensional Gaussian distribution $\mathcal{N}_d(\boldsymbol{\mu}, \boldsymbol{\Sigma})$, then the following set

$$\mathcal{D} := \{\mathbf{X} \mid (\mathbf{X} - \boldsymbol{\mu})^T \boldsymbol{\Sigma}^{-1} (\mathbf{X} - \boldsymbol{\mu}) \leq F_d^{-1}(1 - \alpha)\} \quad (8)$$

specifies the risk domain of \mathbf{X} at risk level α , where F_d^{-1} is the inverse mapping of the cumulative distribution function (CDF) of the chi-squared distribution with d degrees of freedom.

Proof: Since $\mathbf{X} \sim \mathcal{N}_d(\boldsymbol{\mu}, \boldsymbol{\Sigma})$, the probability density function (PDF) of \mathbf{X} takes the following form [24]

$$f(\mathbf{X}) = \frac{1}{(2\pi)^{\frac{d}{2}} |\boldsymbol{\Sigma}|^{\frac{1}{2}}} \exp\left[-\frac{1}{2}(\mathbf{X} - \boldsymbol{\mu})^T \boldsymbol{\Sigma}^{-1} (\mathbf{X} - \boldsymbol{\mu})\right] \quad (9)$$

where $\boldsymbol{\mu} \in \mathbb{R}^d$ and $\boldsymbol{\Sigma} \in \mathbb{R}^{d \times d}$ are the mean and covariance matrix of \mathbf{X} , respectively.

According to the theorem of quadratic distribution [25], a new quadratic random variable derived from \mathbf{X} must obey a one-dimensional chi-squared distribution

$$Q = (\mathbf{X} - \boldsymbol{\mu})^T \boldsymbol{\Sigma}^{-1} (\mathbf{X} - \boldsymbol{\mu}) \sim \chi_d^2, \quad (10)$$

where Q is a quadratic function of \mathbf{X} and χ_d^2 represents the one-dimensional chi-squared distribution with d degrees of freedom.

The CDF of Q is then given by [24]

$$F_d(q) = \Pr(Q \leq q) = P\left(\frac{d}{2}, \frac{q}{2}\right) := p \quad (11)$$

where $P\left(\frac{d}{2}, \frac{q}{2}\right)$ is the regularized gamma function.

As $F_d(q) : R^+ \rightarrow [0, 1]$ is a bijective mapping, we can find the following inverse mapping for $F_d(q)$

$$q = F_d^{-1}(p) : [0, 1] \rightarrow R^+ \quad (12)$$

Given a risk level α (or confidence level $1 - \alpha$), we have $p = 1 - \alpha$, then we can find a value $q_{1-\alpha} = F_d^{-1}(1 - \alpha)$ such that

$$\Pr(Q \leq q_{1-\alpha}) = \Pr(Q \leq F_d^{-1}(1 - \alpha)) = 1 - \alpha \quad (13)$$

According to eq. (10), it follows that the set

$$\{\mathbf{X} \mid (\mathbf{X} - \boldsymbol{\mu})^T \boldsymbol{\Sigma}^{-1} (\mathbf{X} - \boldsymbol{\mu}) \leq q_{1-\alpha} = F_d^{-1}(1 - \alpha)\} \quad (14)$$

forms the risk domain \mathcal{D} of the random variable \mathbf{X} at risk level α . \blacksquare

With Lemma 1, we can now derive the chance constraint for the vehicle to avoid the obstacle. In particular, by restricting our attention to vehicles moving at the same altitude, i.e., $d = 2$, we can find the risk domain \mathcal{D}_{ti} of obstacle i at time t according to Lemma 1, as its location $\mathbf{c}_{ti} \sim \mathcal{N}(\boldsymbol{\mu}_{ti}, \boldsymbol{\Sigma}_i)$. Specifically,

$$\mathcal{D}_{ti} := \{\mathbf{c}_{ti} \mid (\mathbf{c}_{ti} - \boldsymbol{\mu}_{ti})^T \boldsymbol{\Sigma}_i^{-1} (\mathbf{c}_{ti} - \boldsymbol{\mu}_{ti}) \leq F_2^{-1}(1 - \alpha)\} \quad (15)$$

where

$$F_2^{-1}(1 - \alpha) = -2 \ln(\alpha) \quad (16)$$

as

$$F_2(q) = 1 - e^{-\frac{q}{2}} \quad (17)$$

Of note, the boundary of the risk domain \mathcal{D}_{ti} can be geometrically interpreted as a circle or an ellipse, depending on the values of covariance $\boldsymbol{\Sigma}_i$.

To ensure that the probability of collision is smaller than a particular risk level α , the vehicle's location \mathbf{x}_t should be outside the corresponding risk domain \mathcal{D}_{ti} of obstacle i at time t , i.e.,

$$(\mathbf{x}_t - \boldsymbol{\mu}_{ti})^T \boldsymbol{\Sigma}_i^{-1} (\mathbf{x}_t - \boldsymbol{\mu}_{ti}) > F_2^{-1}(1 - \alpha), \quad (18)$$

as

$$\begin{aligned} & \Pr(\text{collision} \mid \text{eq. (18) holds}) \\ &= \Pr(\|\mathbf{c}_{ti} - \mathbf{x}_t\| \leq r_* + r_i = 2\delta \mid \mathbf{x}_t \notin \mathcal{D}_{ti}) \\ &\leq \Pr(\mathbf{c}_{ti} \notin \mathcal{D}_{ti}) \\ &= \Pr((\mathbf{c}_{ti} - \boldsymbol{\mu}_{ti})^T \boldsymbol{\Sigma}_i^{-1} (\mathbf{c}_{ti} - \boldsymbol{\mu}_{ti}) > F_2^{-1}(1 - \alpha)) \\ &= \Pr(Q > q_{1-\alpha}) \\ &= \alpha \end{aligned} \quad (19)$$

In the above inequality, $\Pr(\|\mathbf{c}_{ti} - \mathbf{x}_t\| \leq 2\delta \mid \mathbf{x}_t \notin \mathcal{D}_{ti}) \leq \Pr(\mathbf{c}_{ti} \notin \mathcal{D}_{ti})$ holds because $\delta \rightarrow 0$ (as assumed in the beginning of this subsection), the obstacle would need to be outside of its corresponding risk domain \mathcal{D}_{ti} to meet the collision condition.

Note that the chance constraint in eq. (18) is a deterministic quadratic inequality that is tractable and can be easily implemented, compared with the probabilistic constraint in eq. (19). Moreover, the above discussion can be easily extended to higher dimension problems, such as $d = 3$.

B. Chance Constraints for Multiple Uncertain Obstacles

In this subsection, we consider a more general case where multiple uncertain obstacles (either static or dynamic) are present. The safe ranges for both obstacles and vehicle are still assumed to be negligible.

To attain the chance constraint that ensures the probability of collision with all obstacles doesn't exceed a given threshold ϑ , we apply the same idea presented in the previous subsection. In particular, suppose there are N obstacles, with the location of each obstacle c_{ti} following a two-dimensional Gaussian distribution, i.e., $c_{ti} \sim \mathcal{N}_2(\mu_{ti}, \Sigma_i)$. According to the analysis in the previous subsection, the risk domain \mathcal{D}_{ti} of an obstacle i can be captured by eq. (15), where $\alpha = \vartheta/N$, and probabilistically guaranteed collision avoidance with this obstacle can be ensured by enforcing the deterministic constraint in eq. (18).

To ensure that the probability of collision with any of the obstacles is smaller than the threshold ϑ , the vehicle should avoid the risk domains of all the obstacles at each time step t . This can be achieved by introducing the following constraint

$$(\mathbf{x}_t - \mu_{ti})^T \Sigma_i^{-1} (\mathbf{x}_t - \mu_{ti}) > F_2^{-1}(1 - \alpha) \quad (20)$$

$$\forall i \in \{1, \dots, N\}$$

as

$$\begin{aligned} & \Pr(\text{collision} \mid \text{eq. (20) holds}) \\ &= \Pr\left(\|\mathbf{c}_{ti} - \mathbf{x}_t\| \leq r_* + r_i = 2\delta, \forall i \in \{1, \dots, N\} \mid \mathbf{x}_t \notin \bigcup_{i=1}^N \mathcal{D}_{ti}\right) \\ &\leq \Pr\left(\bigvee_{i=1}^N (\mathbf{c}_{ti} - \mu_{ti})^T \Sigma_i^{-1} (\mathbf{c}_{ti} - \mu_{ti}) > F_2^{-1}(1 - \alpha)\right) \\ &\leq \sum_{i=1}^N \Pr\left((\mathbf{c}_{ti} - \mu_{ti})^T \Sigma_i^{-1} (\mathbf{c}_{ti} - \mu_{ti}) > F_2^{-1}(1 - \alpha)\right) \\ &\leq N\alpha = \vartheta \end{aligned} \quad (21)$$

C. Chance Constraints with Safety Range

In this subsection, we consider the more general case when the safety range of the obstacle/vehicle is non-negligible. For simplicity, the geometric shape of the safety range is assumed to be a time-invariant circle.

As shown in Fig. 1, the radius of the safety range for the obstacle and the vehicle are r_i and r_* , respectively. The possible region \mathcal{X}_{ti} (as defined in eq. (4)) of the obstacle i at time t can be represented by the union of a series of circles with radius r_i , where the circle's center c_{ti} , i.e. the location of the obstacle i , follows a Gaussian distribution. As discussed in Section III-A, we can find the risk domain \mathcal{D}_{ti} for the location c_{ti} of obstacle i at time t according to Lemma 1.

Furthermore, when considering the safety range r_i of obstacle i , the actual risk domain for obstacle i at time step

t is in fact the enveloping area of a series of circles whose centers are inside or on the boundary of the risk domain \mathcal{D}_{ti} . We denote this actual domain as $\mathcal{D}_{ti}^{\text{range}}$, which is a larger area than \mathcal{D}_{ti} as shown in Fig. 1.

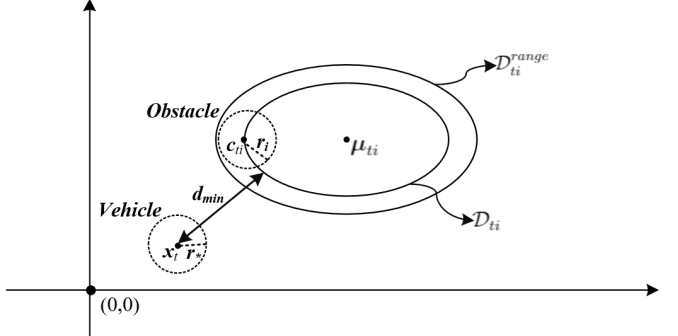


Fig. 1: Schematic of the safety range

Since there is no explicit expression of the actual risk domain $\mathcal{D}_{ti}^{\text{range}}$, we will check the feasibility of the chance constraints by measuring the minimum distance between the vehicle's location \mathbf{x}_t and the risk domain of c_{ti} , which is denoted as d_{\min} . In fact, d_{\min} can be treated as the distance between a point and an ellipse, which can be calculated explicitly according to [26]. Then we check the feasibility of the chance constraints using the inequality

$$d_{\min}(\mathbf{x}_t, \mathcal{D}_{ti}) > r_i + r_* \quad (22)$$

if it holds, then

$$\begin{aligned} & \Pr(\text{collision} \mid \text{eq. (22) holds}) \\ &= \Pr(\|\mathbf{x}_t - \mathbf{c}_{ti}\| \leq r_i + r_j \mid \mathbf{x}_t \notin \mathcal{D}_{ti}^{\text{range}}) \\ &\leq \Pr(\mathbf{c}_{ti} \notin \mathcal{D}_{ti}) \\ &= \alpha \end{aligned} \quad (23)$$

Thus, given a risk level α which denotes the probabilistic bound on the chance that the vehicle collides with any obstacle i at any time step t , we can transform the probabilistic constraint eq. (23) into a deterministic constraint eq. (22) equivalently, in consideration of the safety range of both obstacle and vehicle.

D. Transformation of Relative Uncertainty

So far we have only considered the scenario where obstacle uncertainty exists. In this subsection, we introduce the transformation of **relative uncertainty**, which can reduce both vehicle uncertainty and obstacle uncertainty into one common uncertainty. With this, the risk domain theory established above can then be smoothly extended to scenarios where both forms of uncertainty exist.

For the simplicity of notation, let random variable \mathbf{X} denote the location \mathbf{c}_{ti} of an obstacle i and random variable \mathbf{Y} denote the location \mathbf{x}_t of the vehicle, at time step t . Thus, under the assumption of Gaussian distribution, it follows that

$$\begin{aligned} \mathbf{X} &\sim \mathcal{N}_2((\mu_1, \mu_2)^T, \begin{bmatrix} \sigma_{11} & \sigma_{12} \\ \sigma_{21} & \sigma_{22} \end{bmatrix}) \\ \mathbf{Y} &\sim \mathcal{N}_2((v_1, v_2)^T, \begin{bmatrix} \tau_{11} & \tau_{12} \\ \tau_{21} & \tau_{22} \end{bmatrix}) \end{aligned} \quad (24)$$

Consider that both $\text{Var}(\mathbf{X})$ and $\text{Var}(\mathbf{Y})$ are expressed in a common coordinate system. It follows that the relative random variable $\mathbf{Z} = (\mathbf{X} - \mathbf{Y})$ denotes the relative position with uncertainty between the obstacle and the vehicle. It obeys a new Gaussian distribution [27], which is displayed as

$$\begin{aligned}\mathbf{Z} &\sim \mathcal{N}(\boldsymbol{\mu}, \boldsymbol{\Sigma}) \\ &\sim \mathcal{N}(\mathbf{E}(\mathbf{X} - \mathbf{Y}), \text{Var}(\mathbf{X} - \mathbf{Y}))\end{aligned}\quad (25)$$

where the mean and covariance of \mathbf{Z} are respectively represented by

$$\begin{aligned}\boldsymbol{\mu} &= \mathbf{E}(\mathbf{X} - \mathbf{Y}) \\ &= \mathbf{E}(\mathbf{X}) - \mathbf{E}(\mathbf{Y}) \\ &= (\mu_1 - v_1, \mu_2 - v_2)^T \\ \boldsymbol{\Sigma} &= \text{Var}(\mathbf{X} - \mathbf{Y}) \\ &= \text{Var}(\mathbf{X}) + \text{Var}(\mathbf{Y}) - 2\rho\sqrt{\text{Var}(\mathbf{X})\text{Var}(\mathbf{Y})} \\ &= \begin{bmatrix} \sigma_{11} & \sigma_{12} \\ \sigma_{21} & \sigma_{22} \end{bmatrix} + \begin{bmatrix} \tau_{11} & \tau_{12} \\ \tau_{21} & \tau_{22} \end{bmatrix} \\ &\quad - 2\rho\sqrt{\begin{bmatrix} \sigma_{11} & \sigma_{12} \\ \sigma_{21} & \sigma_{22} \end{bmatrix} \begin{bmatrix} \tau_{11} & \tau_{12} \\ \tau_{21} & \tau_{22} \end{bmatrix}}\end{aligned}\quad (26)$$

and ρ represents the correlation coefficient between the vehicle and the obstacle i .

As a comparison to the aforementioned scenarios where both variances are expressed in a common coordinate system, it is more often to see that $\text{Var}(\mathbf{X})$ is expressed in the body-fixed coordinate system of the obstacle i whereas $\text{Var}(\mathbf{Y})$ is also expressed in its own body-fixed coordinate system of the vehicle respectively. Therefore, it's necessary to perform coordinate transformations before the further transformations of relative uncertainty.

For reference, a ground coordinate system is first established. Relative to the ground coordinate system, we can find the orientation vectors $(\cos \alpha, \sin \alpha)^T$ of the obstacle i and $(\cos \beta, \sin \beta)^T$ of the vehicle respectively at the same time t . Note that now both variances, $\text{Var}(\mathbf{X})$ and $\text{Var}(\mathbf{Y})$, are expressed in their own body-fixed coordinate systems and can be re-expressed in the common ground coordinate system as follows

$$\begin{aligned}\text{Var}(\mathbf{X})' &= \mathbf{J}_{obs} \text{Var}(\mathbf{X}) \mathbf{J}_{obs}^T \\ \text{Var}(\mathbf{Y})' &= \mathbf{J}_{veh} \text{Var}(\mathbf{Y}) \mathbf{J}_{veh}^T\end{aligned}\quad (27)$$

where

$$\begin{aligned}\mathbf{J}_{obs} &= \begin{bmatrix} \cos \alpha & -\sin \alpha \\ \sin \alpha & \cos \alpha \end{bmatrix} \\ \mathbf{J}_{veh} &= \begin{bmatrix} \cos \beta & -\sin \beta \\ \sin \beta & \cos \beta \end{bmatrix}\end{aligned}\quad (28)$$

Therefore, the covariance of \mathbf{Z} expressed in the ground coordinate system, denoted by $\boldsymbol{\Sigma}'$, is displayed as

$$\begin{aligned}\boldsymbol{\Sigma}' &= \text{Var}(\mathbf{X} - \mathbf{Y})' \\ &= \text{Var}(\mathbf{X})' + \text{Var}(\mathbf{Y})' - 2\rho\sqrt{\text{Var}(\mathbf{X})' \text{Var}(\mathbf{Y})'}\end{aligned}\quad (29)$$

For simplicity, the covariance of \mathbf{Z} can be further diagonalized through a coordinate transformation

$$\boldsymbol{\Sigma}'' = \mathbf{U}^T \boldsymbol{\Sigma}' \mathbf{U}\quad (30)$$

where $\boldsymbol{\Sigma}''$ is a diagonal matrix indicating the covariance of \mathbf{Z} , and \mathbf{U} is an orthogonal matrix whose every column vector is the corresponding eigenvector of the inverse matrix of $\boldsymbol{\Sigma}'$. Also, the expected relative position $\boldsymbol{\mu}'' = (m, n)^T$ between the obstacle i and the vehicle takes the following form

$$\boldsymbol{\mu}'' = \mathbf{U}^T (\mu_1 - v_1, \mu_2 - v_2)^T\quad (31)$$

Through the transformation of relative uncertainty as well as coordinate transformation, the relationship between the location of obstacle \mathbf{X} and vehicle \mathbf{Y} can be transformed to the relationship between \mathbf{Z} and origin $(0, 0)$, as shown in Fig. 2. In other words, through the transformation, the original uncertain location of vehicle \mathbf{Y} (vehicle uncertainty) is transformed to be a deterministic location $(0, 0)$ in the new relative coordination system, while its location uncertainty is added to the location uncertainty of the obstacle \mathbf{X} .

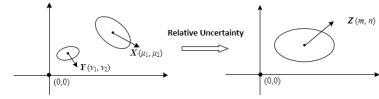


Fig. 2: Schematic of the transformation of relative uncertainty

According to the risk domain theory established in the previous sections III-C, we can also build the risk domain for the relative position \mathbf{Z} between the i th obstacle and the vehicle at time t

$$(\mathbf{Z} - \boldsymbol{\mu}'')^T \boldsymbol{\Sigma}''^{-1} (\mathbf{Z} - \boldsymbol{\mu}'') = F_2^{-1}(1 - \alpha)\quad (32)$$

whose boundary is also a circle or an ellipse.

Similar to eq. (22), to check whether the vehicle would collide with the obstacle, it's only required to check the minimum distance d_{\min} between the origin $(0, 0)$ and the elliptic risk domain eq. (32) whose center is $\boldsymbol{\mu}'' = (m, n)^T$. If d_{\min} is greater than the safety range, the probability of collision will be bounded by the prescribed risk level α .

On the grounds of the discussion of relative uncertainty above, we successfully transform the vehicle and environmental obstacle uncertainties into one common uncertainty, instead of dealing with them separately.

E. Comparison with Other Methods

Zhu et al. [18] linearized their collision conditions to get linear chance constraints and then reformulate them into deterministic constraints in terms of the mean and covariance of the states. Take the inter-robot collision avoidance constraints formulated in their paper as an example. The positions and covariances of two robots are given as $\mathbf{p}_i \sim \mathcal{N}(\hat{\mathbf{p}}_i, \boldsymbol{\Sigma}_i)$, $\mathbf{p}_j \sim \mathcal{N}(\hat{\mathbf{p}}_j, \boldsymbol{\Sigma}_j)$, and r_i, r_j are their safety ranges. The collision condition of robot i with respect to robot j at time t is

$$C_{ij} = \{\mathbf{x}_i : \|\mathbf{p}_i - \mathbf{p}_j\| \leq r_i + r_j\}\quad (33)$$

and then the instant collision probability of robot i and j is

$$\Pr(\mathbf{x}_i \in C_{ij}) = \int_{\|\mathbf{p}_i - \mathbf{p}_j\| \leq r_i + r_j} p(\mathbf{p}_i - \mathbf{p}_j) d(\mathbf{p}_i - \mathbf{p}_j)\quad (34)$$

which is an integral of a multivariate Gaussian probability density function (PDF).

The numerical integral result is the exact collision probability. However, there is no closed form to figure out the collision probability. Zhu et al. obtained an approximated upper bound through the linearization of the collision condition. As shown below, the collision region C_{ij} can be linearized to a half space \tilde{C}_{ij}

$$\tilde{C}_{ij} := \{ \mathbf{x} \mid \mathbf{a}_{ij}^T (\mathbf{p}_i - \mathbf{p}_j) \leq b_{ij} \} \quad (35)$$

such that $C_{ij} \subset \tilde{C}_{ij}$, thus

$$\Pr(\mathbf{x}_i \in C_{ij}) \leq \Pr(\mathbf{x}_i \in \tilde{C}_{ij}) \quad (36)$$

Hence, the original chance constraints can be transformed to linear constraints based on the work of Blackmore et al. [15],

$$\Pr(\mathbf{x}_i \in C_{ij}) \leq \frac{1}{2} + \frac{1}{2} \operatorname{erf} \left(\frac{b_{ij} - \mathbf{a}_{ij}^T (\hat{\mathbf{p}}_i - \hat{\mathbf{p}}_j)}{\sqrt{2\mathbf{a}_{ij}^T (\Sigma_i + \Sigma_j) \mathbf{a}_{ij}}} \right) \quad (37)$$

Furthermore, the linear constraints above can be transformed into deterministic constraints

$$\mathbf{a}_{ij}^T (\hat{\mathbf{p}}_i - \hat{\mathbf{p}}_j) - b_{ij} \geq \operatorname{erf}^{-1}(1 - 2\delta_r) \sqrt{2\mathbf{a}_{ij}^T (\Sigma_i + \Sigma_j) \mathbf{a}_{ij}} \quad (38)$$

In contrast, although the transformation from probabilistic constraints to deterministic ones is also performed in our paper, the key difference is that it is totally not required to perform the approximation of linearization in our proposed method. Instead, through the introduction of risk domain and relative uncertainty transformation in our method, it is convenient to check the probability of collision, which avoids the integral operation in eq. (34), while maintaining the accuracy of collision probability.

IV. CHANCE CONSTRAINED RRT PLANNING

In this section, a novel chance constrained RRT algorithm (CC-RRT) is developed as an extension of the standard RRT algorithm. Through incorporating the chance constraints formulated in section III, this proposed algorithm applies to not only single-vehicle systems but also multi-vehicle systems, subject to vehicle and/or environmental obstacle uncertainties.

Briefly speaking, the standard RRT algorithm is a sampling-based motion planning algorithm [5]. The key idea is to incrementally grow a tree to dynamically generate feasible trajectories [22]. It is particularly suitable for path planning problems involving obstacles. The proposed CC-RRT algorithm extends the standard RRT algorithm to further incorporate probabilistic constraints. Whereas the standard RRT algorithm grows a tree of trajectories known to be feasible, CC-RRT grows a tree known to satisfy a risk bound of collision probability at each node. It means that following the trajectory planned by CC-RRT, the probability that the vehicle collides with obstacles doesn't exceed the prescribed risk level.

Fig. 3 illustrates that the proposed CC-RRT algorithm grows a tree with the purpose of finding a path (red) which satisfies the probabilistic feasibility, connecting the start and goal points. The vehicle uncertainty of the vehicle at each node is represented as a red ellipse, and the obstacle uncertainty is represented as a blue ellipse. Note that the direction of the

long axis of the red ellipse aligns with the segment connecting the last node and current one, which signifies the heading orientation of the vehicle. The vehicle's location at each node is checked against the chance constraints with the nearby obstacles, by using the relative uncertainty transformation in Section III-D. If the constraint doesn't hold, i.e. $d_{min} < r_i + r_*$, it means the probability of collision really exceeds a prescribed value and the current node should be discarded; otherwise, the current node should be reserved and may contribute to growing future paths.

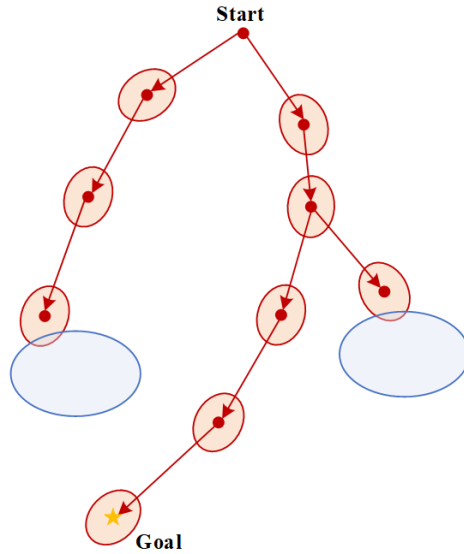


Fig. 3: Diagram of CC-RRT planning

We can use a directed graph $G = (V, E)$ to represent the paths generated by CC-RRT. In that way, a feasible path can be interpreted as a vertex sequence (v_1, v_2, \dots, v_n) , where $v_1 = x_{\text{start}}$ and $v_n = x_{\text{goal}}$. The edge $(v_i, v_{i+1}) \in E$ represents a path connecting two neighbouring nodes.

A. CC-RRT for Single-Vehicle Systems under Uncertainty

1) *Static Obstacles under Uncertainty*: To begin with, consider a simple scenario where all the obstacles present are assumed to be static and uncertain. The steps of CC-RRT planning intended for such a scenario are presented in **Algorithm 1**.

It utilizes the chance constraints formulation developed in section III, which applies a fixed probability bound ϑ/N across all obstacles, leading to deterministic constraints that can be computed at each time step. With the chance constraints formulation, one can determine whether equivalent deterministic constraints are satisfied or not through evaluating the relative position between a sample point x_{rand} and the corresponding risk domain \mathcal{D}_i of obstacle i for all time steps at a given risk level α . The sample point x_{rand} is a node of the CC-RRT tree that doesn't violate the risk domain \mathcal{D}_i . It is guaranteed that each node of the tree satisfies the probability bound of collision with any obstacle i through CC-RRT planning.

2) *Dynamic Obstacles under Uncertainty*: Based on Algorithm 1, we proceed to consider a more complicated scenario

Algorithm 1 CC-RRT Static Obstacles under Uncertainty

```

1: Vertex  $V \leftarrow \mathbf{x}_{\text{start}}$ , Edge  $E \leftarrow \emptyset$ , Iteration step  $k \leftarrow 0$ ;
2: Construct tree  $G$  by using  $V$  and  $E$ ;
3: while  $k < \text{max}$  do
4:   Randomly pick a location  $\mathbf{x}_{\text{rand}}$ ;
5:   Find the node  $\mathbf{x}_{\text{nearest}}$  in the tree  $G$  that is the nearest to  $\mathbf{x}_{\text{rand}}$ ;
6:   Generate a new node  $\mathbf{x}_{\text{new}}$  out of the tree  $G$ ;
7:   Generate a new path  $\mathbf{p}_{\text{new}}$  between  $\mathbf{x}_{\text{nearest}}$  and  $\mathbf{x}_{\text{new}}$ ;
8:   if  $\text{NoIntersect}(\mathbf{p}_{\text{new}}, \mathcal{D}_i)$ 
9:     Add the new node  $\mathbf{x}_{\text{new}}$  to tree  $G$ ;
10:    Add the new path  $\mathbf{p}_{\text{new}}$  to tree  $G$ ;
11:    if  $\|\mathbf{x}_{\text{new}} - \mathbf{x}_{\text{goal}}\| < \delta$ 
12:      break;
13:    end if
14:  end if
15:   $k \leftarrow k + 1$ ;
16: end while

```

where dynamic obstacles subject to uncertainty are present. In particular, in this scenario, the risk domain \mathcal{D}_{ti} of obstacle i varies over time. Such time dependence allows the inclusion of dynamic obstacles.

To address this scenario, we just need to figure out the risk domain \mathcal{D}_{ti} of dynamic obstacle i at a particular time step t . The dynamic obstacle then can be viewed as a static obstacle at the same time step. In doing so, we can generalize what we conclude in section **IV-A1** here. Specifically, we can determine whether equivalent deterministic constraints are satisfied or not by evaluating the relative position between a sample point \mathbf{x}_{rand} and the corresponding risk domain \mathcal{D}_{ti} of obstacle i at this time step t . Moving forward to the next time step $t + 1$, the same evaluation process can be performed again to check whether the probability of collision exceeds the prescribed risk bound. However, different from section **IV-A1** where \mathcal{D}_i is constant for the static obstacle, here the risk domain \mathcal{D}_{ti} for the dynamic obstacle is time-varying. Thus, \mathcal{D}_{ti} at last time step t should be updated by $\mathcal{D}_{(t+1)i}$ at current time step $t + 1$.

Another concern is that in most cases, the sequence number of a new node in the generated tree is inconsistent with the number of time steps, because a parent node in the tree may have more than one descendant nodes. To address this issue, we use the minimal steps from the new node to the start point, rather than the sequence number, to be corresponding with the number of time steps.

The procedure is presented in **Algorithm 2**.

B. CC-RRT for Multi-vehicle Systems under Uncertainty

1) *Fixed Planning Order Strategy*: For safe flying of a multi-vehicle system, in addition to avoid environmental obstacles, the possibility of collision between any two vehicles also needs to be considered. This can be addressed by decomposing the problem into a set of single-vehicle path planning sub-problems, with each sub-problem solved in a pre-fixed iterative order by the algorithm of path planning.

Particularly, at the beginning of every new time step, when we are ready to extend the trajectory for a particular vehicle in the multi-vehicle system, the possible trajectories for any other vehicles within the same time step may have yet to be determined. In view of this, for the particular vehicle being prepared to be planned, the positions of other vehicles within

Algorithm 2 CC-RRT Dynamic Obstacles under Uncertainty

```

1: Vertex  $V \leftarrow \mathbf{x}_{\text{start}}$ , Edge  $E \leftarrow \emptyset$ , Iteration step  $k \leftarrow 0$ ;
2: Construct tree  $G$  by using  $V$  and  $E$ ;
3: while  $k < \text{max}$  do
4:   Randomly pick a location  $\mathbf{x}_{\text{rand}}$ ;
5:   Find the node  $\mathbf{x}_{\text{nearest}}$  in the tree  $G$  that is the nearest to  $\mathbf{x}_{\text{rand}}$ ;
6:   Generate a new node  $\mathbf{x}_{\text{new}}$  out of the tree  $G$  between  $\mathbf{x}_{\text{nearest}}$  and  $\mathbf{x}_{\text{rand}}$ ;
7:   Generate a new path  $\mathbf{p}_{\text{new}}$  between  $\mathbf{x}_{\text{nearest}}$  and  $\mathbf{x}_{\text{new}}$ ;
8:   Find minimum steps  $m$  from  $\mathbf{x}_{\text{nearest}}$  to  $\mathbf{x}_{\text{start}}$ ;
9:   Minimum steps from  $\mathbf{x}_{\text{new}}$  to  $\mathbf{x}_{\text{start}}$   $m \leftarrow m + 1$ ;
10:  Find current time step  $t$  corresponding to  $m$ ;
11:  Find risk domain  $\mathcal{D}_{ti}$  of obstacle  $i$  at current time step  $t$ ;
12:  if  $\text{NoIntersect}(\mathbf{p}_{\text{new}}, \mathcal{D}_i)$ 
13:    Add the new node  $\mathbf{x}_{\text{new}}$  to tree  $G$ ;
14:    Add the new path  $\mathbf{p}_{\text{new}}$  to tree  $G$ ;
15:    if  $\|\mathbf{x}_{\text{new}} - \mathbf{x}_{\text{goal}}\| < \delta$ 
16:      break;
17:    end if
18:  end if
19:   $k \leftarrow k + 1$ ;
20: end while

```

current time step are uncertain. Thus, when we perform CC-RRT algorithms given in **Algorithm 2** to generate new path for a particular vehicle in the system, all the other vehicles can be formulated as dynamic obstacles obeying a probability distribution. In doing so, the multi-vehicle path planning problem is reduced to a set of single-vehicle sub-problems. To further reduce the risk for one vehicle to collide with the other vehicles in the team, we consider the uncertainties of vehicles at not only the current time step but also the next few steps.

The procedure of this fixed planning order strategy for a multi-vehicle system are presented in **Algorithm 3** (Take a team consisting of three vehicles a, b, c as a demo).

Algorithm 3 Multi-CC-RRT Fixed Planning Order

```

1: Start point  $a_0 \leftarrow a_{\text{start}}$ ,  $b_0 \leftarrow b_{\text{start}}$ ,  $c_0 \leftarrow c_{\text{start}}$ ;
   Current time step  $t \leftarrow 0$ ;
2: while  $t < \text{max}$  do
3:    $\text{path\_}a\text{.append}(a_t)$ ,  $\text{path\_}b\text{.append}(b_t)$ ,
    $\text{path\_}c\text{.append}(c_t)$ ;
4:    $\text{ObstacleList\_}a \leftarrow [b_t, b_{t+1}, b_{t+2}, c_t, c_{t+1}, c_{t+2}]$ ;
5:    $[a_{t+1}, a_{t+2}, a_{t+3}] \leftarrow \text{CC-RRT}(\text{ObstacleList\_}a)$ ;
6:    $\text{ObstacleList\_}b \leftarrow [a_{t+1}, a_{t+2}, a_{t+3}, c_t, c_{t+1}, c_{t+2}]$ ;
7:    $[b_{t+1}, b_{t+2}, b_{t+3}] \leftarrow \text{CC-RRT}(\text{ObstacleList\_}b)$ ;
8:    $\text{ObstacleList\_}c \leftarrow [a_{t+1}, a_{t+2}, a_{t+3}, b_{t+1}, b_{t+2}, b_{t+3}]$ ;
9:    $[c_{t+1}, c_{t+2}, c_{t+3}] \leftarrow \text{CC-RRT}(\text{ObstacleList\_}c)$ ;
10:  if  $\|a_{t+1} - a_{\text{goal}}\| < \delta$  or  $\|b_{t+1} - b_{\text{goal}}\| < \delta$  or
     $\|c_{t+1} - c_{\text{goal}}\| < \delta$ 
    break;
11: end if
12:  $t \leftarrow t + 1$ ;
13: end while

```

2) Updated Planning Order and Temporary Stop Strategy:

In section **IV-B1**, the fixed planning order strategy only ensures that the decisions taken by individual vehicles do not conflict. However, the fixed order update rule ignores any substantial benefit from replanning order for each vehicle in the team, which could result in unnecessary total traffic delays. An extension to the strategy mentioned above is presented here in the form of an updated planning order. This new approach relies on the measurement of the steps of the planned path to goal for any individual vehicle in the team, which reflects a vehicle's motivation to replan rather than cycling through vehicles in order.

At each iteration, a permit is used to identify which vehicle can carry out CC-RRT algorithm given in **Algorithm 2** firstly. Every individual vehicle evaluates its motivation in a bid to be the permit holder. When the current permit holder finishes planning, it passes the permit to the next vehicle with the greatest motivation, and so on. This procedure generates an updated planning order where vehicles that may benefit the most from replanning order can do so sooner, without waiting for other vehicles which have little motivation to replan. Note that if a vehicle updates its plan, the respective constraints imposed on the other vehicles must also be updated accordingly. Most often, the vehicle that is closest to its goal will typically generate the highest motivation, allowing it to complete its task sooner and then can be arranged to receive a new task, which improves the efficiency in terms of resource allocation. Moreover, this strategy can reduce the computation intensity and air traffic density, since once an individual vehicle achieves its goal, it can be removed from the team with no further path plannings needed.

It doesn't necessarily mean that the vehicle with the greatest motivation can always quickly find the path to its goal. In fact, sometimes it even fails to find a feasible path for such a vehicle, due to the presence of other vehicles formulated as dynamic obstacles. To make a compensation, the strategy of temporary stop for the vehicle can be introduced. Specifically, we introduce temporary stop nodes along the vehicle's path where it can safely stop for one or more time steps in a bid to yield to other vehicles in the team. This not only saves computational time but also lowers the risk of collision with other vehicles.

The procedure of updated planning order and temporary stop strategy is presented in **Algorithm 4**.

Algorithm 4 Updated Planning Order and Temporary Stop

```

1: Current time step  $k$ ;
2: Pass permit to the vehicle that is the closest to its goal;
3: while vehicle  $i$  is active do
4:   Perform CC-RRT to identify a path  $p_k^*$  satisfying all constraints;
5:   if current vehicle owns permit
6:     if iteration  $< max$ 
7:       Generate a new path for the current vehicle;
8:     else
9:       Temporary stop for the current vehicle;
10:    end if
11:    Pass permit to the next vehicle with the best motivation;
12:  else
13:    Evaluate the motivation for the current vehicle;
14:  end if
15:   $i \leftarrow i + 1$ 
16: end while

```

V. SIMULATION STUDY

In this section, several simulation cases are evaluated to verify the probabilistic feasibility of the proposed CC-RRT algorithms using a single UAV or multiple UAVs. The proposed algorithms were implemented in Python and simulations were run on an Intel Core i7 1.90GHz laptop with 16GB of RAM.

A. Experimental Setup

All the obstacles (either static or dynamic) in this section are assumed to be uncertain and safety ranges are assumed to

be circles. The radius of the safety range is set to $r = 0.3$ for the environmental obstacles and $r = 0.1$ for the UAVs. The static obstacle is located at $\mathbf{X}_{sobs} = (x, y) \sim \mathcal{N}(\boldsymbol{\mu}_{sobs}, \boldsymbol{\Sigma}_{sobs})$ with $\boldsymbol{\mu}_{sobs} = (3, 3)$ and $\boldsymbol{\Sigma}_{sobs} = [\frac{1}{6} \ 0; \ 0 \ \frac{1}{24}]$. The dynamic obstacle is located at $\mathbf{X}_{dobs} = (x, y) \sim \mathcal{N}(\boldsymbol{\mu}_{dobs}, \boldsymbol{\Sigma}_{dobs})$ with $\boldsymbol{\Sigma}_{dobs} = [\frac{1}{6} \ 0; \ 0 \ \frac{1}{24}]$, while $\boldsymbol{\mu}_{dobs}$ is a time-varying parameter determined by its known trajectory for all time steps. For the simplicity of notation, we denote all the covariances here as $\boldsymbol{\Sigma}$. The position of the UAV is set to $\mathbf{X}_{uav} = (x, y) \sim \mathcal{N}(\boldsymbol{\mu}_{uav}, \boldsymbol{\Sigma}_{uav})$ with $\boldsymbol{\Sigma}_{uav} = [\frac{1}{24} \ 0; \ 0 \ \frac{1}{96}]$, while the UAV's position is time-varying and determined by the nodes of path planned by the CC-RRT at each time step t .

For a given risk level α in each case, the simulation is divided into two stages:

1) **Stage I: CC-RRT Planning**

- Formulate chance constraints for every obstacle i at every time step t at the given risk level α .
- Run CC-RRT to find a path with the desired probabilistic feasibility for each UAV in the system.

2) **Stage II: Validation with Random Trials**

- Given a planned path, generate random points from the associated distribution, which represent the realization of each obstacle i and the UAV at every time step t .
- Check whether the planned path under the given risk level α for the UAV given in stage I collides with each realized obstacle i whose location is generated randomly at every time step t .
- Perform random trials for 100 times for each risk level α under the current case. Count the number of collision occurrence.

B. Case 1: Static Uncertain Obstacle + Single Deterministic UAV

In this case, a static uncertain obstacle and a single deterministic UAV are considered.

Fig. 4a-4c demonstrate sample paths generated by our proposed CC-RRT at $\alpha = 0.20$, $\alpha = 0.10$, and $\alpha = 0.05$ respectively under the same covariance $\boldsymbol{\Sigma}$. The red line indicates the planned path, the blue circle or ellipse indicates the risk domain of the static obstacle, and the yellow circle indicates the realized position of the static obstacle with safety range in a random trial. As shown in Tab. I, the path planned by our proposed CC-RRT can ensure that the probability of collision with the static obstacle at any time step t does not exceed α .

Tab. II compares the performances of different planning algorithms with different levels of covariances under the same risk level $\alpha = 0.05$. It illustrates that compared with traditional RRT which doesn't consider chance constraints, our proposed CC-RRT and Zhu's method of linearization [18] both effectively identify probabilistically feasible paths for the vehicle in the presence of a static, uncertain obstacle. Thanks to the tighter bound offered by our proposed method than the method of linearization, our method achieves the same level of safety guarantee with the shorter length of trajectory. The efficiency

of our method becomes more significant as the covariance increases.

C. Case 2: Static Uncertain Obstacle + Single Uncertain UAV

In this case, a static uncertain obstacle and a single uncertain UAV are considered.

Fig. 5a-5c depict paths generated by CC-RRT at three risk levels $\alpha = 0.20$, $\alpha = 0.10$, and $\alpha = 0.05$ respectively. Here, the red ellipse indicates the risk domain of the vehicle due to its vehicle uncertainty, others are the same with Case 1. The transformation of relative uncertainty is applied to convert both risk domains of the vehicle and the static obstacle into a common one. The simulation results under different risk levels with the same covariance Σ are summarized in Tab. I, which illustrates that the proposed CC-RRT can effectively identify a probabilistically feasible path for the vehicle in the presence of both vehicle uncertainty and static obstacle uncertainty. Similar to Case 1, Tab. II indicates that as compared to Zhu's method of linearization and traditional RRT planning without chance constraints at the same risk level $\alpha = 0.05$, our method generates shorter paths while satisfying the safety requirement.

D. Case 3: Dynamic Uncertain Obstacle + Single Uncertain UAV

In this case, two obstacles are considered. One is static and the other one is dynamic. Both obstacles and the UAV are subject to uncertainties.

Fig. 6a visualizes the procedure of CC-RRT path planning at a particular time step when $\alpha = 0.05$. The green ellipse which moves forward represents the risk domain of the dynamic obstacle while the blue one represents the risk domain of the static obstacle. The red line is the planned trajectory at the current time step and the light blue lines are the explored trajectories. In Fig. 6b, the red line indicates the final trajectory of the vehicle planned by CC-RRT, and the newly added green ellipse indicates the risk domain of the dynamic obstacle at all time steps. Moreover, the transformation of relative uncertainty is applied to convert risk domains of both the vehicle and the static/dynamic obstacle into a common one. Clearly, our proposed method can also handle the dynamic obstacle in uncertain environment. Tab. I summarizes the simulation results under different risk levels with respect to the same covariance Σ . In general, lower risk level produces more conservative solutions with less collision chance and longer paths, which is well demonstrated in all above three cases. Our chance constrained method provides a quantitative bound to balance the risk and efficiency. Furthermore, Tab. II suggests that our method achieves a good balance between the efficiency and safety.

E. Case 4: Multiple Uncertain UAVs + Fixed Planning Order

In this case, the CC-RRT planning for a system consisting of three UAVs in the presence of a static obstacle is studied. The positions of both the UAVs and the static obstacle obey the pre-defined Gaussian distributions with time-varying means.

The CC-RRT planning is carried out with the risk level set to $\alpha = 0.05$. As shown in Fig. 7a, when performing CC-RRT

for a vehicle, the other two vehicles are viewed as dynamic obstacles at the current time step, and their uncertainties at the current time step as well as the next two steps are considered based on their previous step's planning, which are shown as green and purple ellipses. Those three look-ahead steps help reduce the risk of collision in the future. In Fig. 7b, the red, purple and green lines indicate the paths generated by CC-RRT for three vehicles in the team respectively.

F. Case 5: Multiple Uncertain UAVs + Updated Planning Order + Temporary Stop

To improve the efficiency of multi-vehicle path planning with CC-RRT, two new features, updated order and temporary stop, are introduced in this case as a comparison to the strategy of fixed planning order employed in Case 4, under the same risk level $\alpha = 0.05$ and the same covariance level Σ . The maximum iteration is set to 500. If the trajectory is identified within the maximum iteration steps, we deem it a feasible CC-RRT path planning. The values are only computed from successful runs.

Fig. 8a shows that according to the updated planning order, the vehicle (the red point) which is closest to its goal, i.e., (10, 5), will perform path planning earlier than the other vehicles in the team. Fig. 8b shows such a possibility that although a vehicle (the red point) is the permit holder, its possible way to the goal point may be blocked by the other vehicles (black ellipses) in the team or the environmental obstacles, which makes it hard to find a feasible way (the red line). By applying the temporary stop strategy, such a vehicle can stop for a while (one time step or more) to yield to the other vehicles, which increases feasibility and saves computational time.

Fig. 8c shows a scenario where a vehicle has already reached its goal, and thus can be removed from the system (only black ellipses need to be considered), which eases the traffic density. The black, purple and green line in Fig. 8d represent the paths generated by the CC-RRT algorithm for all three vehicles in the team at all time steps. Tab. III illustrates that compared with the fixed planning order strategy in Case 4, this strategy can greatly reduce the length of the trajectory and increase the success rate of CC-RRT path planning for the operation of a multi-vehicle system.

TABLE III: Efficiency and Safety of Two Strategies of CC-RRT

Strategy	Path Found	Avg. Length	Avg. Chance of Collision
Fixed Order	5/10	37.5	4%
Updated Order+Temp Stop	9/10	27.4	2%

VI. CONCLUSIONS

In this paper, a novel chance constrained RRT algorithm (CC-RRT) together with chance constraints formulation for location uncertainty is presented for a team of vehicles, which allows for either static or dynamic uncertain obstacles. Through converting possible regions of obstacles into corresponding risk domains, the probabilistic constraints can be transformed

TABLE I: Efficiency and Safety of CC-RRT under Different Risk Levels

Case #	Algorithm	α	Avg. Length	Avg. Chance of Collision
Case 1	CC-RRT	0.20	18.1	7%
		0.10	18.6	4%
		0.05	20.9	3%
Case 2	CC-RRT	0.20	18.4	5%
		0.10	20.3	2%
		0.05	21.7	1%
Case 3	CC-RRT	0.20	21.4	6%
		0.10	24.8	3%
		0.05	26.2	2%

TABLE II: Efficiency and Safety of Planning Algorithms under Different Covariance Levels (L: Avg. trajectory length; CC: Avg. chance of collision; CT: Avg. computational time)

Case #	Algorithm	1/4 Σ			Σ			4 Σ		
		L	CC	CT	L	CC	CT	L	CC	CT
Case 1	CC-RRT	19.2	3%	16.6ms	20.9	3%	18.8ms	22.1	4%	22.4ms
	Linearization[18]	21.7	2%	17.0ms	22.9	3%	19.2ms	25.3	3%	23.5ms
	RRT	15.4	52%	15.2ms	16.3	57%	15.2ms	20.5	65%	15.2ms
Case 2	CC-RRT	19.5	1%	19.3ms	21.7	1%	22.5ms	24.2	3%	26.7ms
	Linearization[18]	22.0	1%	20.5ms	23.8	1%	24.0ms	26.5	2%	27.9ms
	RRT	16.3	51%	18.2ms	17.2	53%	18.2ms	21.4	62%	18.2ms
Case 3	CC-RRT	23.5	1%	341.1ms	26.2	2%	385.6ms	29.1	3%	457.1ms
	Linearization[18]	26.4	1%	359.8ms	28.5	1%	435.2ms	30.6	2%	548.9ms
	RRT	20.7	51%	311.2ms	21.6	55%	311.2ms	25.9	68%	311.2ms

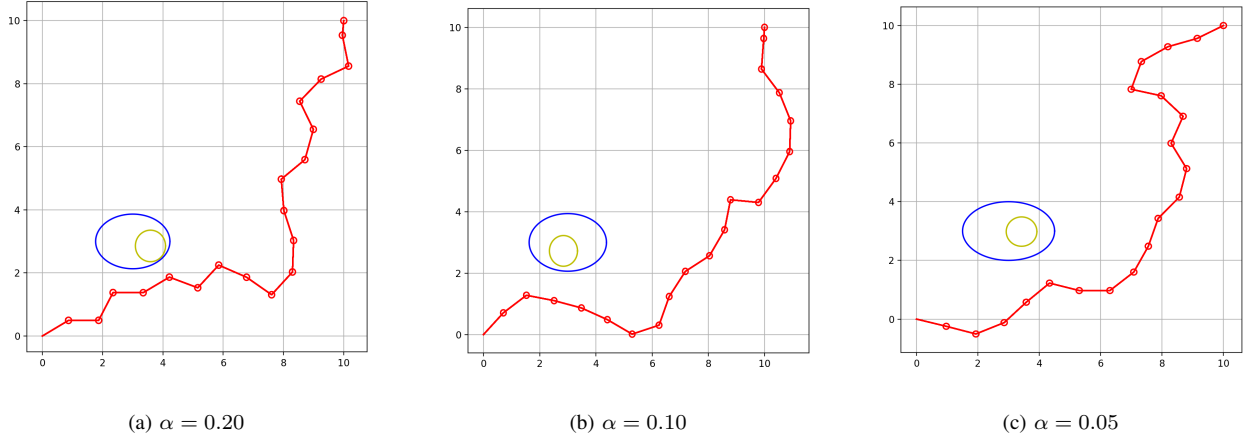


Fig. 4: Case 1 Static Uncertain Obstacle + Single Deterministic UAV

into deterministic ones. Also, through the introduction of relative uncertainty, this approach can be applied to scenarios where both vehicle and environmental obstacle uncertainties exist. Simulation results show that the paths generated by the proposed CC-RRT algorithm are probabilistically feasible in terms of avoiding collisions, and are shorter than the ones generated by the state-of-the-art algorithms.

ACKNOWLEDGMENTS

This work was supported partially by San Diego State University under the University Grants Program, and partially by the National Science Foundation under Grants CNS-1953048/1730589 and ECCS-1953049/1839707.

REFERENCES

- [1] D. P. Thipphavong, R. Apaza, B. Barmore, V. Battiste, B. Burian, Q. Dao, M. Feary, S. Go, K. H. Goodrich, J. Homola, *et al.*, “Urban air mobility airspace integration concepts and considerations,” in *2018 Aviation Technology, Integration, and Operations Conference*, 2018, p. 3676.
- [2] S. Sawadsitang, D. Niyato, P.-S. Tan, and P. Wang, “Joint ground and aerial package delivery services: A stochastic optimization approach,” *IEEE Transactions on Intelligent Transportation Systems*, vol. 20, no. 6, pp. 2241–2254, 2018.
- [3] D. González, J. Pérez, V. Milanés, and F. Nashashibi, “A review of motion planning techniques for automated ve-

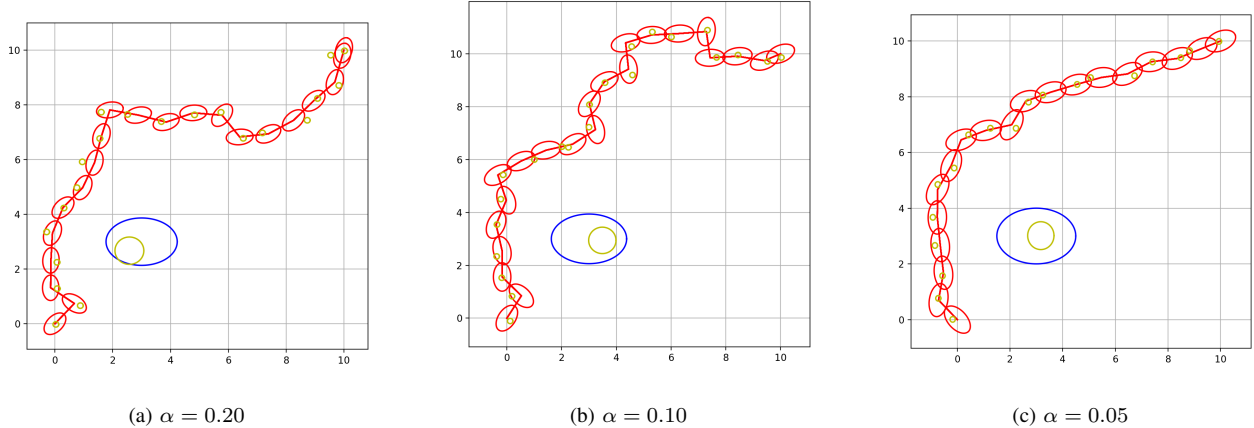


Fig. 5: Case 2 Static Uncertain Obstacle + Single Uncertain UAV

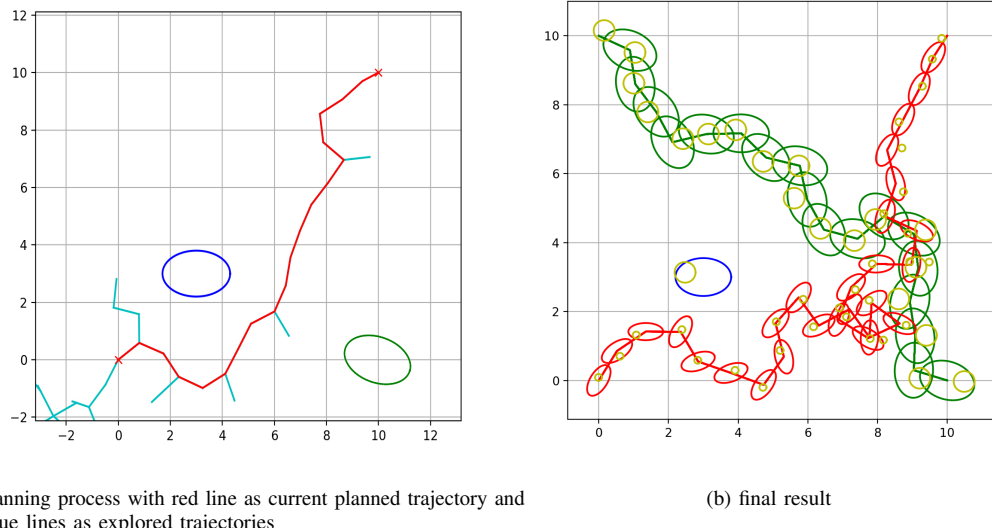


Fig. 6: Case 3 Dynamic Uncertain Obstacle + Single Uncertain UAV

hicles,” *IEEE Transactions on Intelligent Transportation Systems*, vol. 17, no. 4, pp. 1135–1145, 2015.

[4] Y. Lin and S. Saripalli, “Sampling-based path planning for UAV collision avoidance,” *IEEE Transactions on Intelligent Transportation Systems*, vol. 18, no. 11, pp. 3179–3192, 2017.

[5] S. M. LaValle, *Planning algorithms*. Cambridge university press, 2006.

[6] S. Thrun, “Probabilistic robotics,” *Communications of the ACM*, vol. 45, no. 3, pp. 52–57, 2002.

[7] Y. Yang, J. Zhang, K.-Q. Cai, and M. Prandini, “Multi-aircraft conflict detection and resolution based on probabilistic reach sets,” *IEEE Transactions on Control Systems Technology*, vol. 25, no. 1, pp. 309–316, 2016.

[8] T. Lew, R. Bonalli, and M. Pavone, “Chance-constrained sequential convex programming for robust trajectory optimization,” in *2020 European Control Conference (ECC)*, IEEE, 2020, pp. 1871–1878.

[9] S. Prentice and N. Roy, “The belief roadmap: Efficient planning in linear pomdps by factoring the covariance,” in *Robotics research*, Springer, 2010, pp. 293–305.

[10] R. Pepy and A. Lambert, “Safe path planning in an uncertain-configuration space using rrt,” in *2006 IEEE/RSJ International Conference on Intelligent Robots and Systems*, IEEE, 2006, pp. 5376–5381.

[11] B. Luders, M. Kothari, and J. How, “Chance constrained rrt for probabilistic robustness to environmental uncertainty,” in *AIAA guidance, navigation, and control conference*, 2010, p. 8160.

[12] P. Li, M. Wendt, and G. Wozny, “A probabilistically constrained model predictive controller,” *Automatica*, vol. 38, no. 7, pp. 1171–1176, 2002.

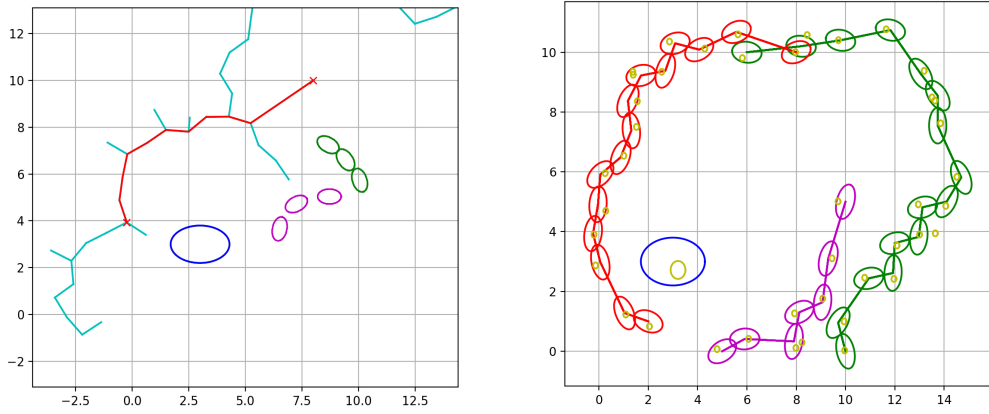


Fig. 7: Case 4 Multiple Uncertain UAVs + Fixed Planning Order

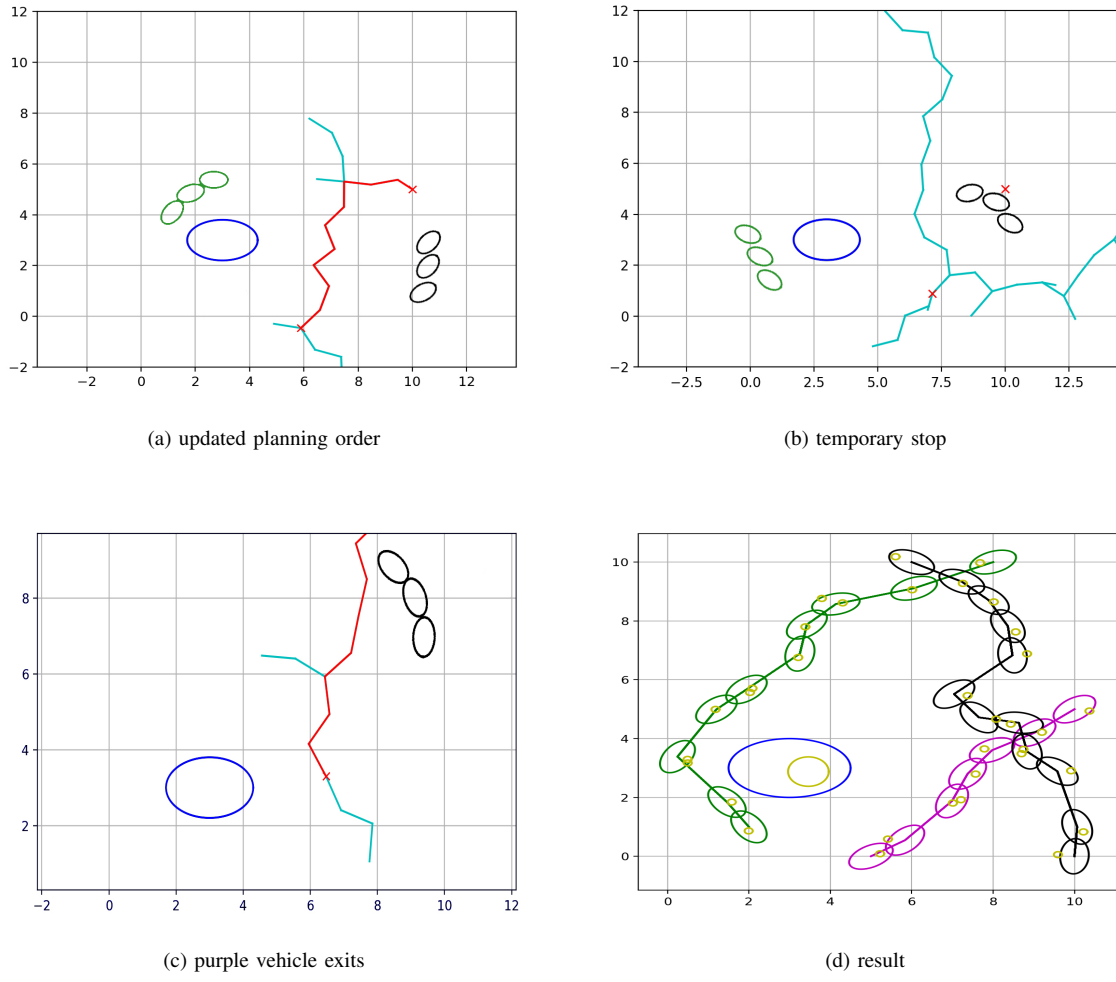


Fig. 8: Case 5 Multiple Uncertain UAVs + Updated Planning Order + Temporary Stop

- [13] J. Chen, l. Chen, and D. Sun, “Air traffic flow management under uncertainty using chance-constrained optimization,” *Transportation Research Part B: Methodological*, vol. 102, pp. 124–141, 2017.
- [14] L. Blackmore, M. Ono, A. Bektassov, and B. C. Williams, “A probabilistic particle-control approximation of chance-constrained stochastic predictive control,” *IEEE transactions on Robotics*, vol. 26, no. 3, pp. 502–517, 2010.
- [15] L. Blackmore, M. Ono, and B. C. Williams, “Chance-constrained optimal path planning with obstacles,” *IEEE Transactions on Robotics*, vol. 27, no. 6, pp. 1080–1094, 2011.
- [16] N. Du Toit, “Robot motion planning in dynamic, cluttered, and uncertain environments: The partially closed-loop receding horizon control approach,” Ph.D. dissertation, California Institute of Technology, 2010.
- [17] M. Castillo-Lopez, P. Ludvig, S. A. Sajadi-Alamdar, J. L. Sanchez-Lopez, M. A. Olivares-Mendez, and H. Voos, “A real-time approach for chance-constrained motion planning with dynamic obstacles,” *IEEE Robotics and Automation Letters*, vol. 5, no. 2, pp. 3620–3625, 2020.
- [18] H. Zhu and J. Alonso-Mora, “Chance-constrained collision avoidance for mavs in dynamic environments,” *IEEE Robotics and Automation Letters*, vol. 4, no. 2, pp. 776–783, 2019.
- [19] P. Scerri, S. Owens, B. Yu, and K. Sycara, “A decentralized approach to space deconfliction,” in *2007 10th international conference on information fusion*, IEEE, 2007, pp. 1–8.
- [20] O. Purwin and R. D’Andrea, “Path planning by negotiation for decentralized agents,” in *2007 American Control Conference*, IEEE, 2007, pp. 5296–5301.
- [21] V. R. Desaraju and J. P. How, “Decentralized path planning for multi-agent teams in complex environments using rapidly-exploring random trees,” in *2011 IEEE International Conference on Robotics and Automation*, IEEE, 2011, pp. 4956–4961.
- [22] S. M. LaValle, “Rapidly-exploring random trees: A new tool for path planning,” 1998.
- [23] Y. Liu, “A progressive motion-planning algorithm and traffic flow analysis for high-density 2d traffic,” *Transportation Science*, vol. 53, no. 6, pp. 1501–1525, 2019.
- [24] R. Vershynin, *High-dimensional probability: An introduction with applications in data science*. Cambridge university press, 2018, vol. 47.
- [25] H. Hotelling, “The generalization of student’s ratio,” in *Breakthroughs in statistics*, Springer, 1992, pp. 54–65.
- [26] V. A. Zorich, *Mathematical analysis II*. Springer, 2016.
- [27] T. A. Snijders, *Multilevel analysis*. Springer, 2011.